High-Power Ferromagnetic Resonance without a Degenerate Spin-Wave Manifold

R. D. McMichael and P. E. Wigen
Department of Physics, The Ohio State University, Columbus, Ohio 43210
(Received 20 October 1989)

The nonlinear dynamics of the main magnetoexchange branch of a circular thin (0.45 μm) film of yttrium iron garnet are investigated at perpendicular resonance. Distinct "fingers of auto-oscillation" arise from each magnetoexchange mode in the low-power spectrum. A set of equations of motion derived from a microscopic Hamiltonian are integrated to compare with experiment. In the first finger, the model predicts the power for onset of auto-oscillation to within 1 dB of the experiment and the frequency to within 15%.

PACS numbers: 76.50.+g, 05.45.+b

The topic of nonlinear mechanics has been and continues to be a growing area of research applicable across many fields of science. In particular, nonlinear magnetic systems have been a fruitful field of study in recent years. In this paper, we report on the nonlinear behavior of a normally magnetized magnetic thin film, and on a model of this system which has produced results of unprecedented precision.

A number of observations of auto-oscillations and chaos have been reported in bulk ferromagnets under parallel pumping and perpendicular pumping both at the subsidiary resonance and at the main resonance.[1-11] However, in all of these experiments an entire manifold of degenerate spin waves is excited, severely complicating the dynamics of the system.[12] The normal approach to the analysis involves the S theory[13] of spin-wave interactions which in turn is truncated by considering only a selected few of the very large number of degenerate modes available to the system.[14] This produces a severe limitation to the analysis and at best only qualitative agreement is obtained between models and the experimental data in bulk samples.[10,15,16]

In the case of a thin film magnetized normally to its surface, however, the "uniform" precession mode falls at the bottom of the spin-wave band and the normal modes of the system are not a continuous spectrum of spin waves, but are magnetoexchange modes with discrete frequencies due to the boundary conditions.[17] By adjusting the sample dimensions, the frequencies of the normal modes can be adjusted to vary from a high density of normal modes to a condition having a very low density of well separated modes.

In this paper we report the results of investigations into high-power resonance effects in a thin-film sample with a low density of normal modes. Then we will present our theoretical model, which does not require the severe truncation procedures associated with the S theory,[13,14] and show the favorable comparison of the predictions of our model with the experiments.

Experiments have been performed on several samples etched from a 3.0-μm-thick film of yttrium iron garnet deposited on a gadolinium-gallium-garnet substrate. The data described here come from experiments performed on a circular sample with a diameter of 0.6 mm and a thickness of 0.45 μm, inferred from the measured diameter and the magnetoexchange-mode spacing in the low-power spectrum. The sample was placed in a TE_{102} cavity of a standard reflection-type spectrometer operating at 9.242 GHz. The maximum microwave power available at the cavity is 41 mW, and will be referred to as 0 dB. The temperature of the cavity was stabilized at 285 K in a cryostat using liquid nitrogen.

The low-power absorption spectrum of the main magnetoexchange branch is shown in Fig. 1(a). Not visible in this figure are two very weak resonances located 30 and 87 Oe downfield from the origin of the main branch

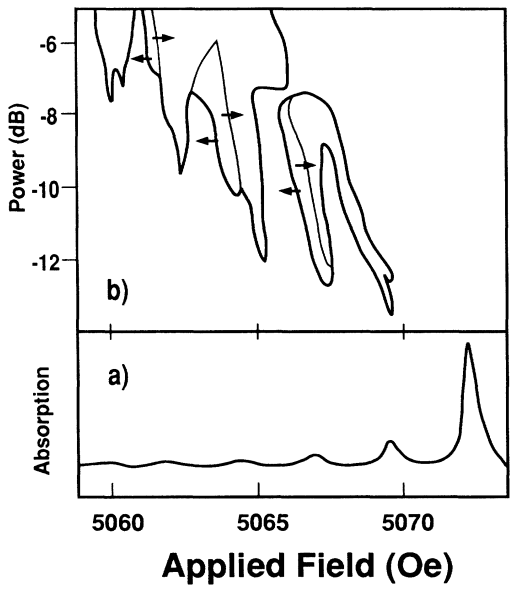

FIG. 1. (a) Low-power spectrum of yttrium-iron-garnet film 0.45 μm thick and 0.6 mm in diameter. (b) Fingers of auto-oscillation and chaos at higher powers. Hysteretic onset of auto-oscillation is indicated by arrows and narrow lines within the finger boundaries.

which are interpreted as the $n=2$ and 3 exchange branches. The weak intensities of these branches indicate that the spins are nearly free at the surfaces of the film, and the appearance of the $n=2$ branch indicates that the pinning conditions are not identical at the two surfaces of the film. The half-widths of the low-power resonances in the main branch are about 0.3 Oe.

High-power effects in the magnetoexchange modes were observed by sweeping the applied field at fixed power levels separated by 0.5-dB intervals. As the pump power is increased, the first indication of nonlinear behavior is the onset of foldover effects where individual modes exhibit hysteretic absorption curves with two stable states, one with a large precession amplitude and the other with a precession amplitude as much as an order of magnitude smaller. The onset of foldover can be seen in the asymmetric line shape of the main mode in Fig. 1(a).

At still higher pump power, the modes begin to auto-oscillate in certain ranges of the applied field. In Fig. 1(b), the domain of time-dependent behavior is outlined. In this study, no attempt was made to differentiate between regular oscillations and chaos, although both regular oscillations and broad-band chaos were observed. The domain of time-dependent behavior is divided into regions we have called "fingers" which are associated with each mode in the low-power spectrum. The fingers at lower applied fields are observed to go into auto-oscillation at higher power levels as the intensities of the associated modes are weaker.

The onset of auto-oscillation along the low-field boundaries of the fingers is often hysteretic in a manner similar to that of foldover. For example, at -10 dB with increasing applied field, oscillations in the second finger are not observed until the thinner line with the rightward pointing arrow is crossed at about 5066.8 Oe. If the applied field is then decreased, the oscillations persist until the line with the leftward pointing arrow is crossed at about 5066.2 Oe.

The first (highest field) finger has a behavior quite different from the rest of the fingers in that it is only observed when the main resonance is in a low-amplitude foldover state. At the high-field boundary of the first finger, the first mode makes a transition to a high-amplitude foldover state and the oscillations cease. If the field is then decreased, the oscillations are not observed until the first mode drops back to its low-amplitude state, usually well downfield from the first finger. Auto-oscillation frequencies and pumping powers at the onset of auto-oscillation in the first four fingers are listed in Table I.

Within 1 or 2 dB of the onset power in a finger, the character of the oscillation does not usually change dramatically. At higher power levels, however, smaller domains with quite different behavior are observed within the region outlined in Fig. 1(b). Transitions between these different smaller domains occur as the applied field or the pumping power is varied, and are sometimes hysteretic, making complete characterization of the system difficult at the highest powers.

TABLE I. Auto-oscillation frequencies and incident power levels at onset for the fingers observed in the experiment and in the model.

	Frequency (MHz)		Onset power (dB)	
Finger No.	Expt.	Model	Expt.	Model
1	4.61	3.97	−13.5	−14.3
2	5.22	4.07	−13	−7.6
3	16.2	12.3	−12	−9.0
4	15.0	3.74	−9.5	−10.3

The Hamiltonian, $\mathcal{H}$, is made up of the following terms:

$$\mathcal{H}=\mathcal{H}_{Zee}+\mathcal{H}_{\text{demag}}+\mathcal{H}_{dd}+\mathcal{H}_{\text{pump}}. \tag{1}$$

The first term, $\mathcal{H}_{Zee}=-H_0M_z$ is the interaction of the magnetization, $\mathbf{M}$, with the static applied field, $\mathbf{H}_0$, which is applied perpendicular to the surface of the film in a direction that we will define to be the z direction. The second term, $\mathcal{H}_{\text{demag}}=2\pi M_z^2$, is the interaction of the magnetization with the shape demagnetization field in the film. The third term represents the magnetostatic and exchange splitting of the magnetoexchange modes, and the fourth term represents the interaction with the microwave-frequency pumping field.

The Hamiltonian is written in terms of the canonical variables a and a^*, defined by

$$M^+=M_x+iM_y=a(2\gamma M_s-\gamma^2aa^*)^{1/2}, \tag{2}$$

$$M_z=M_s-\gamma aa^*, \tag{3}$$

where γ is the gyromagnetic ratio, $16.7\times10^6\ \mathrm{G^{-1}s^{-1}}$. This is the classical analog of the Holstein-Primakoff transformation.[18] Of course, a will have some spatial dependence and therefore it is expanded in terms of orthogonal functions $m_i(\mathbf{r})$ for the ith mode appropriate to the sample geometry, so that

$$a=\sum_i a_i m_i(\mathbf{r}), \tag{4}$$

and

$$\int_v d\mathbf{r}\, m_i^*(\mathbf{r})m_j(\mathbf{r})=v\delta_{ij}, \tag{5}$$

where v is the volume of the sample. When the Hamiltonian is written in terms of this expansion of a, and an integration is performed over the sample volume, the first three terms of the Hamiltonian become

$$\mathcal{H}=\text{const}+\gamma\sum_i(H_0-4\pi M_s+D_{ii})a_i^*a_i$$

$$+2\pi\gamma^2\sum_{ijkl}A_{ijkl}a_i^*a_j^*a_ka_l, \tag{6}$$

where

$$A_{ijkl} = \frac{1}{v}\int_v d\mathbf{r}\, m_i^*(\mathbf{r}) m_j^*(\mathbf{r}) m_k(\mathbf{r}) m_l(\mathbf{r}) \tag{7}$$

and D_{ii} represents the resonant field shift of mode i due to magnetostatic and exchange splitting.

The equations of motion of the variables a_i can be found from the Hamiltonian by the relation

$$\dot{a}_i = -i\,\partial\mathcal{H}/\partial a_i^* . \tag{8}$$

It is convenient to make a transformation to a slowly varying set of unitless variables, c_i, such that $a_i = (M_s/2\gamma)^{1/2} c_i e^{-i\omega t}$. Making this change of variables and ignoring terms which oscillate at angular frequencies of 2ω, the equations of motion become

$$\frac{dc_i}{dt} = -i\gamma\left[(H_0 - H_i^{\mathrm{res}} - i\Gamma)c_i + \frac{h^p}{2} I_i^* + 2\pi M_s \sum_{jkl} A_{ijkl} c_j^* c_k c_l\right], \tag{9}$$

where $H_i^{\mathrm{res}} = \omega/\gamma + 4\pi M_s - D_{ii}$, Γ is the half-width of the low-power resonances included to model damping, h^p is the amplitude of the linearly polarized pumping field, and

$$I_i = v^{-1}\int_v d\mathbf{r}\, m_i(\mathbf{r}) \tag{10}$$

is the normalized transverse dipole moment of the ith mode.

These are the equations of motion which are used to model the behavior of the interacting magnetoexchange modes. All of the parameters in these equations can be obtained from first principles and compared with the low-power resonance curves, or calculated from the spatial dependence of the various modes.

Using parameters appropriate for the sample, the equations of motion for the first four modes visible in the low-power spectrum were integrated numerically using a Runge-Kutta fifth- and sixth-order algorithm. The linewidths and resonant fields of the modes were taken from the low-power spectrum, and the resonant fields were offset by 5062.3 Oe, recognizing that only field differences are important in Eq. (9). The interaction parameters and mode intensities were calculated assuming that the modes have Bessel-function spatial dependence. The equations of motion exhibit foldover at moderate powers, and time-dependent behavior in fingers at higher powers. A plot showing the domain of time-dependent behavior in the model is shown in Fig. 2. Hysteresis of the type shown in Fig. 1(b) along the downfield boundaries of the fingers is observed, but for simplicity, the domain of time-dependent behavior is indicated only for increasing applied field.

The frequencies and input power levels at the onset of auto-oscillation in the model are listed with the experimental values in Table I. The frequencies of the first two fingers are within 15% of the experimental frequencies, and the power level of the first finger is in excellent agreement with the experiment. Results of similar quality have also been obtained for the first finger of auto-oscillation in other thin-film samples with similar aspect ratios. However, the agreement between experiment and theory on onset power levels does not extend to the other fingers. Comparison with a three-mode model shows that the presence of a fourth mode suppresses auto-oscillation in the third finger, suggesting that the low onset power of the fourth and possibly the third finger in the model may be an effect of truncating the model to a few modes.

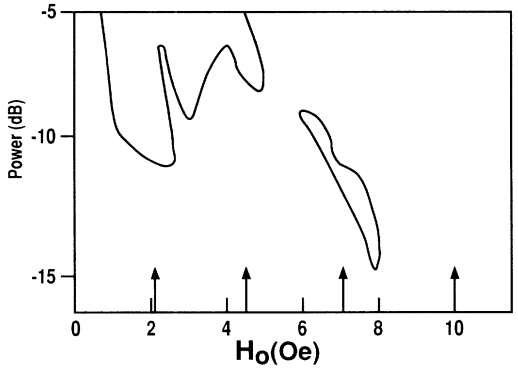

FIG. 2. Fingers of auto-oscillation in a model of the first four modes appearing in the low-power spectrum. The resonant-field values, offset by 5062.3 Oe, are indicated by the vertical arrows. The frequency of auto-oscillation at the onset of the first finger is within 15% of the experimental frequency.

Because of the limited number of modes in a thin film with frequencies near the main resonance, the task of modeling the system is much simpler than the corresponding task in the bulk samples, and this is reflected in the quality of the results. The model predicts foldover and auto-oscillations which, for the first time, are in the correct frequency range and in the correct range of pumping power. The first finger appears to be particularly well modeled with an onset power within 1 dB and a frequency within 15% of the experimental values. We believe this to be the most accurate calculation of an auto-oscillation frequency in a magnetic system yet published.

From the somewhat higher onset powers predicted from the model for the lower-field fingers, it is clear that the model is not yet complete. The model has not incorporated those normal modes of the film that belong to the main branch, but do not couple to the driving field. These modes, which have a higher density at lower fields, may contribute to the dynamics through a process analogous to a second-order Suhl instability.[19] For example, a pair of modes with resonant fields between the first and second modes in the low-power spectra may account for the splitting observed in the first finger and other modes

may account for the difference between our model and experiment in the other fingers. Research in this area is underway.

[1]T. S. Hartwick, E. R. Peresinni, and M. T. Weiss, J. Appl. Phys. **32**, 223S (1961).

[2]W. Wettling, W. D. Wilber, P. Kabos, and C. E. Patton, Phys. Rev. Lett. **51**, 1680 (1983).

[3]H. Yamazaki, J. Phys. Soc. Jpn. **53**, 1155 (1984).

[4]G. Gibson and C. Jeffries, Phys. Rev. A **29**, 811 (1984).

[5]M. Mino and Y. Yamazaki, J. Phys. Soc. Jpn. **55**, 4168 (1986).

[6]F. M. de Aguiar and S. M. Rezende, Phys. Rev. Lett. **56**, 1070 (1986).

[7]A. I. Smirnov, Zh. Eksp. Teor. Fiz. **90**, 385 (1986) [Sov. Phys. JETP **63**, 222 (1986)].

[8]H. Yamazaki, M. Mino, H. Nagashima, and M. Warden, J. Phys. Soc. Jpn. **56**, 742 (1987).

[9]P. Bryant, C. Jeffries, and K. Nakamura, Phys. Rev. Lett. **60**, 1185 (1988).

[10]P. Bryant, C. Jeffries, and K. Nakamura, Phys. Rev. A **38**, 4223 (1988).

[11]T. L. Carroll, L. M. Pecora, and F. J. Fachford, Phys. Rev. A **40**, 377 (1989).

[12]X. Y. Zhang and H. Suhl, Phys. Rev. B **38**, 4893 (1988).

[13]V. E. Zakharov, V. S. L'vov, and S. S. Starobinets, Usp. Fiz. Nauk **114**, 609 (1974) [Sov. Phys. Usp. **17**, 896 (1975)].

[14]K. Nakamura, S. Ohta, and K. Kawasaki, J. Phys. C **15**, L143 (1982).

[15]X. Y. Zhang and H. Suhl, Phys. Rev. A **32**, 2530 (1985).

[16]S. M. Rezende, O. F. de Alcantra Bonfim, and F. M. de Aguiar, Phys. Rev. B **33**, 5153 (1986).

[17]M. Sparks, Phys. Rev. B **1**, 3831 (1970).

[18]T. Holstein and H. P. Primakoff, Phys. Rev. **58**, 1098 (1940).

[19]H. Suhl, J. Phys. Chem. Solids **1**, 209 (1957).